

Fiber-optic system for monitoring fast photoactivation dynamics of optical highlighter fluorescent proteins

Zhiguo Pei,^{1,2} Lingsong Qin,^{1,2} Zhihong Zhang,^{1,2} Shaoqun Zeng,^{1,2}
and Zhen-Li Huang^{1,2,*}

¹*Britton Chance Center for Biomedical Photonics, Wuhan National Laboratory for Optoelectronics-Huazhong University of Science and Technology, Wuhan 430074, China*

²*Key Laboratory of Biomedical Photonics of Ministry of Education, Huazhong University of Science and Technology, Wuhan 430074, China*

*leo@mail.hust.edu.cn

Abstract: Characterizing the photoactivation performance of optical highlighter fluorescent proteins is crucial to the realization of photoactivation localization microscopy. In contrast to those fluorescence-based approaches that require complex data processing and calibration procedures, here we report a simple and quantitative alternative, which relies on the measurement of small absorption spectra changes over time with a fiber-optic system. Using Dronpa as a representative highlighter protein, we have investigated the capacity of this system in monitoring the fast photoactivation process.

© 2011 Optical Society of America

OCIS codes: (120.6200) Spectrometers and spectroscopic instrumentation; (300.1030) Absorption

References and links

1. S. W. Hell, "Far-field optical nanoscopy," *Science* **316**(5828), 1153–1158 (2007).
2. B. Huang, H. Babcock, and X. Zhuang, "Breaking the diffraction barrier: super-resolution imaging of cells," *Cell* **143**(7), 1047–1058 (2010).
3. E. Betzig, G. H. Patterson, R. Sougrat, O. W. Lindwasser, S. Olenych, J. S. Bonifacino, M. W. Davidson, J. Lippincott-Schwartz, and H. F. Hess, "Imaging intracellular fluorescent proteins at nanometer resolution," *Science* **313**(5793), 1642–1645 (2006).
4. H. Shroff, C. G. Galbraith, J. A. Galbraith, and E. Betzig, "Live-cell photoactivated localization microscopy of nanoscale adhesion dynamics," *Nat. Methods* **5**(5), 417–423 (2008).
5. P. Kanchanawong, G. Shtengel, A. M. Pasapera, E. B. Ramko, M. W. Davidson, H. F. Hess, and C. M. Waterman, "Nanoscale architecture of integrin-based cell adhesions," *Nature* **468**(7323), 580–584 (2010).
6. J. Liu, Z. G. Pei, L. Wang, Z. H. Zhang, S. Q. Zeng, and Z. L. Huang, "A straightforward and quantitative approach for characterizing the photoactivation performance of optical highlighter fluorescent proteins," *Appl. Phys. Lett.* **97**(20), 203701 (2010).
7. F. V. Subach, G. H. Patterson, S. Manley, J. M. Gillette, J. Lippincott-Schwartz, and V. V. Verkhusha, "Photoactivatable mCherry for high-resolution two-color fluorescence microscopy," *Nat. Methods* **6**(2), 153–159 (2009).
8. G. Patterson, M. Davidson, S. Manley, and J. Lippincott-Schwartz, "Superresolution imaging using single-molecule localization," *Annu. Rev. Phys. Chem.* **61**(1), 345–367 (2010).
9. R. Ando, H. Mizuno, and A. Miyawaki, "Regulated fast nucleocytoplasmic shuttling observed by reversible protein highlighting," *Science* **306**(5700), 1370–1373 (2004).
10. S. Habuchi, R. Ando, P. Dedecker, W. Verheijen, H. Mizuno, A. Miyawaki, and J. Hofkens, "Reversible single-molecule photoswitching in the GFP-like fluorescent protein Dronpa," *Proc. Natl. Acad. Sci. U.S.A.* **102**(27), 9511–9516 (2005).

11. S. Habuchi, P. Dedecker, J.-i. Hotta, C. Flors, R. Ando, H. Mizuno, A. Miyawaki, and J. Hofkens, "Photo-induced protonation/deprotonation in the GFP-like fluorescent protein Dronpa: mechanism responsible for the reversible photoswitching," *Photochem. Photobiol. Sci.* **5**(6), 567–576 (2006).
 12. C. Flors, J.-i. Hotta, H. Uji-i, P. Dedecker, R. Ando, H. Mizuno, A. Miyawaki, and J. Hofkens, "A stroboscopic approach for fast photoactivation-localization microscopy with Dronpa mutants," *J. Am. Chem. Soc.* **129**(45), 13970–13977 (2007).
 13. E. Pastrana, "Fast 3D super-resolution fluorescence microscopy," *Nat. Methods* **8**(1), 46 (2011).
 14. N. Irwin and K. A. Janssen, *Molecular Cloning: a Laboratory Manual*, 3ed., J. Argentine and N. Irwin, eds. (Cold Spring Harbor Laboratory Press, New York 2001).
 15. "CCD noise sources and signal-to-noise ratio," <http://learn.hamamatsu.com/articles/ccdsnr.html>, accessed Mar. 2011.
 16. "HL-2000 tungsten halogen light sources," <http://www.oceanoptics.com/Products/hl2000.asp>, accessed Mar. 2011.
 17. "USB2000+ Miniature Fiber Optic Spectrometer," <http://www.oceanoptics.com/Products/usb2000+.asp>, accessed Mar. 2011.
 18. S. W. Smith, *The Scientist and Engineer's Guide to Digital Signal Processing*, 2nd ed. (California Technical Publishing, 2003).
 19. M. Andresen, A. C. Stiel, S. Trowitzsch, G. Weber, C. Eggeling, M. C. Wahl, S. W. Hell, and S. Jakobs, "Structural basis for reversible photoswitching in Dronpa," *Proc. Natl. Acad. Sci. U.S.A.* **104**(32), 13005–13009 (2007).
 20. *Ocean Optics* catalog (Ocean Optics, Inc., 2011).
 21. A. R. Faro, V. Adam, P. Carpentier, C. Darnault, D. Bourgeois, and E. de Rosny, "Low-temperature switching by photoinduced protonation in photochromic fluorescent proteins," *Photochem. Photobiol. Sci.* **9**(2), 254–262 (2010).
-

1. Introduction

Zooming into living cells with unprecedented spatial resolution is now made possible with the use of various super-resolution microscopy techniques [1,2]. Among them, an intrinsically wide-field imaging approach called photoactivation localization microscopy (PALM) is receiving intensive attention in the field of live cell imaging for its simultaneously long imaging time and large field of view [3–5].

However, PALM relies heavily on a unique class of fluorescence probe, the optical highlighter fluorescent proteins (FPs). In particular, the photoactivation performance of highlighter FPs, such as the photoactivation contrast (determined by the fluorescence signal over background) and the photoactivation/ photobleaching rates, which play a crucial role in the realization of PALM [6,7]. Therefore, it is necessary to produce, study and optimize highlighter FPs with enhanced photoactivation performance in all the above aspects [8]. It is preferable to develop quantitative methods for monitoring the photoactivation dynamics of highlighter FPs, because these parameters are dynamic and are susceptible to the environment. This should be beneficial in the evaluation and screening of highlighter FPs.

Nowadays, monitoring the photoactivation dynamics of highlighter proteins is performed mainly on fluorescence-based approaches, which rely on surveying the changes in fluorescence intensity during photoactivation [6,7]. However, results obtained through these fluorescence-based approaches are relative to the system setup, and the experimental apparatus for measuring the fluorescence is usually very complex making the calibration problematic. Unsurprisingly, researchers are now trying to develop alternative methods for characterizing the photoactivation dynamics. For example, other research groups [9–11] have successfully demonstrated that this could be done by measuring the absorption spectral changes of highlighter FPs over time. This absorption-based approach is surely a promising alternative to the fluorescence-based one, since the measurement and data processing of absorption spectra are much easier and more robust than its fluorescence counterpart. Unfortunately, the experimental set-ups were mainly based on commercial UV-Vis spectrophotometers, and the photoactivation control and absorption spectra measurement were carried out separately and manually. Therefore, photoactivation dynamics could only be measured with time resolution at

minutes level, which cannot meet the current need of fast PALM where the photoactivation occurs preferably within one second [12,13].

Here we report the construction of a system based on a commercial fiber-optic spectrometer for monitoring fast photoactivation dynamics. The performance of this system was characterized and discussed using a representative highlighter fluorescent protein, Dronpa, which was reported to have fast response to photoactivation light [6].

2. Experimental

2.1. Sample preparation

Recombinant Dronpa protein was expressed in *Escherichia coli*. The protein was purified with Ni-NTA chromatography (GE Heath, USA) [14], dialyzed into phosphate-buffered saline (PBS, 8.0 g NaCl, 3.58 g Na₂HPO₄·12H₂O, 0.2 g KCl, 0.24 g KH₂PO₄ dissolved in 1 L distilled water, pH 7.4), diluted with 70% sucrose solution to obtain the final stock solution at the concentration of 1.8×10^{-5} M. In further experiments, a $2 \times 10 \times 45$ mm³ quartz cuvette containing 200 μ L of the stock solution was used.

2.2. Optical setup

First, the frequency of the output of a commercial mode-locked femtosecond Ti:sapphire laser (Mai Tai BB, Spectra Physics, USA) operating at 800 nm was frequency doubled by a second harmonic generation (SHG) crystal (BBO, Castech, China), and then passed through a 650 nm short pass filter (SP650, DHC, China) to remove residual fundamental laser (Fig. 1). The trans-

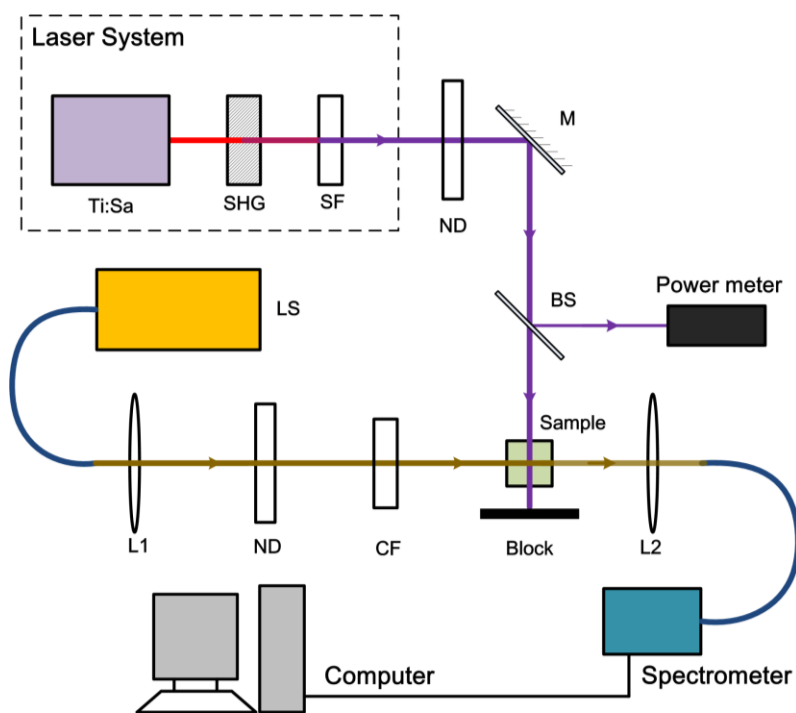


Fig. 1. The optical set-up for monitoring fast photoactivation dynamics. SHG, BBO crystal; SF, short pass filter; ND, neutral density filters; M, mirror; BS, beam splitter; LS, light source; L, focusing lens; CF, color filters; Block, beam block.

mitted SHG laser (400 nm) was attenuated by neutral density filters and split into two orthogonal beams by a glass slide. The intensity of the weaker (reflected) beam was monitored by a commercial power meter (PD300, Ophir, Israel). The stronger (transmitted) beam was used to activate the sample solution in a quartz cuvette polished on all four sides.

The absorption spectra of the same solution were measured in an optical path perpendicular to the photoactivation light. A tungsten-halogen light source (HL-2000-FHSA-LL, Ocean Optics, USA) was guided by a fiber (P400-2-UV-Vis, Ocean Optics, USA), collimated by a glass lens (focal length = 10 mm), attenuated by neutral filters, modulated by a color filter (QB2, Yinxing Optical, China) and a 650 nm short pass filter (SP650, DHC, China), and then used as the light source of the absorption spectra measurement. The transmitted tungsten-halogen light was focused into a fiber (P100-2-UV-Vis, Ocean Optics, USA) by an objective (25x, NA = 0.40, DHC, China) and measured by a miniature fiber-optic spectrometer (USB2000+ , Ocean Optics, USA). Note that the light entered the spectrometer without an entrance slit, collimated by an SAG+UPG mirror onto a 600 lines/mm groove density grating blazed at 500 nm (Ocean Optics grating #3), focused successively by another SAG+UPG mirror, a cylindrical detector collection lens and a OFLV-350-1000 variable long pass order-sorting filter onto a Sony ILX511 CCD array detector with 2048 pixels. The recorded data were saved by an operating software called 'SpectraSuite' (Ocean Optics, USA) and analyzed in Matlab R2009b.

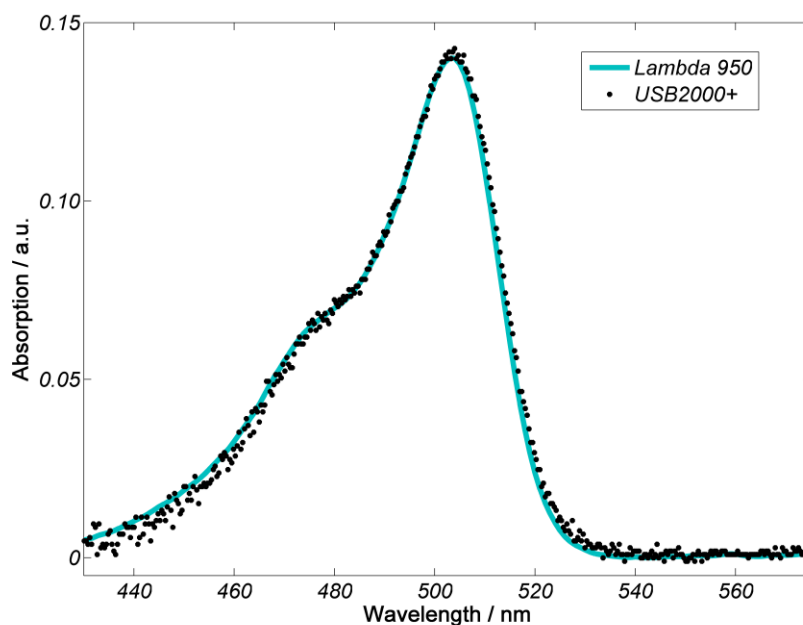


Fig. 2. The absorption spectra of Dronpa measured with a commercial Lambda 950 spectrophotometer and our system based on a USB2000+ miniature fiber-optic spectrometer.

3. Results and discussion

3.1. Measuring the absorption spectrum of Dronpa

The absorption spectrum of Dronpa solution was measured with our fiber-optic system and compared to the results from a commercial spectrophotometer (Lambda 950, PerkinElmer, USA). As shown in Fig. 2, the two spectra overlap nicely, which demonstrates excellent accuracy in both wavelength and intensity of our fiber-optic system.

The wavelength accuracy of our system could be attributed to the fact a careful wavelength calibration using a mercury argon calibration light source (CAL-2000, Ocean Optics, USA) was performed prior to any absorption spectra measurements. However, it was found that the selection and inclusion of suitable color filters into the optical setup (for example, QB2 and SP650 in this study, see Fig. 1) is crucial to guarantee the intensity accuracy.

To understand the role of the color filter used in the setup, it is necessary to begin with a widely used parameter for quantifying the performance of an optoelectronic device, the signal-to-noise ratio (SNR). It is well-known that SNR is defined as the power ratio of signal to the noise corrupting the signal. In our case, the main cause of noise is from the output fluctuation of the light source (HL-2000-FHSA-LL tungsten-halogen lamp) and the noise of the detector (USB2000+ miniature spectrometer). Since the light intensity is attenuated by ND filters (see Fig. 1), the noise from the light source (N_{LS}) equals to the product of the power of light (S) and its power stability (a). Thus N_{LS} = a × S. Meanwhile, the noise of the spectrometer is from its photo-electronic detector, which is a linear array CCD. As outlined previously [15], the noise of the CCD (N_{CCD}) can be described by the following formula:

$$N_{CCD} = \sqrt{S + Dt + N_r^2} \quad (1)$$

where S is the signal, D is the dark current, t is the integration time, and N_r represents the read noise. In our experiment, since the signal reaches at almost the full scale of the detector, the dark noise and the read noise could be safely ignored. Noticing that the contributions of the light source and the detector to the noise are statistically independent, and considering signal averaging (n) between acquisitions, the SNR of the system becomes

$$SNR_{sys} = \frac{nS}{\sqrt{(naS)^2 + nS}} = \frac{1}{\sqrt{a^2 + \frac{1}{nS}}} \quad (2)$$

From Eq. (2), it is shown that the SNR of the system could be optimized by increasing the number of signal averaging (n) and the signal level (S), while the maximum SNR is the reciprocal of the power stability (a) of the light source. Using the HL2000 tungsten-halogen lamp (a = 0.5%) as the light source [16], the maximum SNR was calculated to be 200. However, in our experiments, although the signal (S) from the USB2000+ miniature spectrometer could easily reach its upper detection limit (~6 × 10⁴ counts) [17] with a good combination on the integration time and ND filters, the number of signal averaging (n) is limited to the desired time resolution of the setup, since it was designed to monitor dynamic absorption changes. Considering a time resolution of less than one second and using a typical integration time of 100 ms, the number of signal averaging was set to be 5 in all the experiments. In this case, the maximum SNR (SNR_{sys}^{max}) was calculated to be 188. If the number of signal averaging is more than 5, SNR_{sys}^{max} increases slightly while the time resolution degrades rapidly.

To estimate the minimum resolvable absorption, it is necessary to begin with the definition of absorption:

$$\begin{aligned}
A(\lambda) &= -\log_{10} \left(\frac{I(\lambda)}{I_0(\lambda)} \right) = -\log_{10} \left(1 - \frac{\Delta I(\lambda)}{I_0(\lambda)} \right) \\
&= -\ln \left(1 - \frac{\Delta I(\lambda)}{I_0(\lambda)} \right) / \ln 10 \\
&\approx -0.43 \times \ln \left(1 - \frac{\Delta I(\lambda)}{I_0(\lambda)} \right)
\end{aligned} \tag{3}$$

where I_0 and I represent the intensity of the incident and the transmitted lights, respectively. $\Delta I = I_0 - I$ is the total light intensity variance during the transmission. From Eq. (3), it is obvious that the minimum measurable absorption (A_{\min}), or sensitivity (ΔA), is determined by the accuracy of $\Delta I/I_0$ measurements. Note, that when the SNR falls below 1.0, the signal could not be detected [18]. As a result, the minimum measurable ΔI_{\min} equals to the noise of the system at the intensity level of I_0 , and the value of $\Delta I_{\min}/I_0$ is the reciprocal of the SNR of the absorption spectra measurement system. In our experiment, when the value of $\Delta I_{\min}/I_0$ approaches zero, Eq. (3) could then be approximated as

$$A_{\min}(\lambda) = \Delta A(\lambda) \approx 0.43 \frac{\Delta I_{\min}(\lambda)}{I_0(\lambda)} = \frac{0.43}{SNR_{sys}^{max}} \tag{4}$$

Since $SNR_{sys}^{max} = 188$, the minimum measurable absorption (A_{\min}) was calculated to be 2.29×10^{-3} .

However, the sensitivity (minimum measurable absorption) that is estimated above is only valid for the wavelength region with the strongest signal. Since the absorption spectrum typically covers a broad wavelength range, it is thus necessary to take into account the inhomogeneous output of the tungsten-halogen lamp and estimate those wavelengths with weaker signals. The output of the HL2000 tungsten-halogen lamp is shown in Fig. 3a. Note that the spectral sensitivity of the grating and the CCD detector inside the USB2000+ spectrometer distorted the output profile of the lamp, which should emit with increasing intensity from 300 nm to 2000 nm [16]. Since we are interested in measuring the absorption spectrum of Dronpa whose absorption maximum is located at 503 nm [9], it is necessary to use appropriate filters to shift the maximum output of the lamp from 600 nm to shorter wavelengths. In fact, in our set-up a combination of a color filter QB2 and a 650 nm short pass filter was used, therefore, the signal (S) in the wavelength range from 440 nm to 650 nm is higher than 1×10^4 counts (see Fig. 3b and 3c). With setting the number of signal averaging to 5, the SNR in this wavelength range is calculated to be higher than 149, corresponding to a minimum measurable absorption of 2.89×10^{-3} .

3.2 Monitoring the light-activated trans-cis isomerization of Dronpa

It has previously been reported, that upon minimal illumination at 405 nm, Dronpa can be light-activated from the dark trans state to the fluorescence cis state, in which the 503 nm absorption peak dominates [19]. However, Dronpa in PBS solution displays an absorption maximum at 503 nm and a minor peak at 388 nm, indicating that the UV light-driven cis-trans isomerization of the chromophore is actually accompanied by complex conformational changes [10]. To better monitor this cis-trans photo-isomerization, the Dronpa solution was pretreated with a 473 nm laser (80 mW/cm^2) using a solid state laser (MXL-III-473, CNI) for about 15 minutes. Under these conditions, the fluorescence of Dronpa solution was significantly reduced

and the absorption at 503 nm reaches a minimum ($A = 0.04$, see the spectrum with lowest absorption in 503 nm in Fig. 4a).

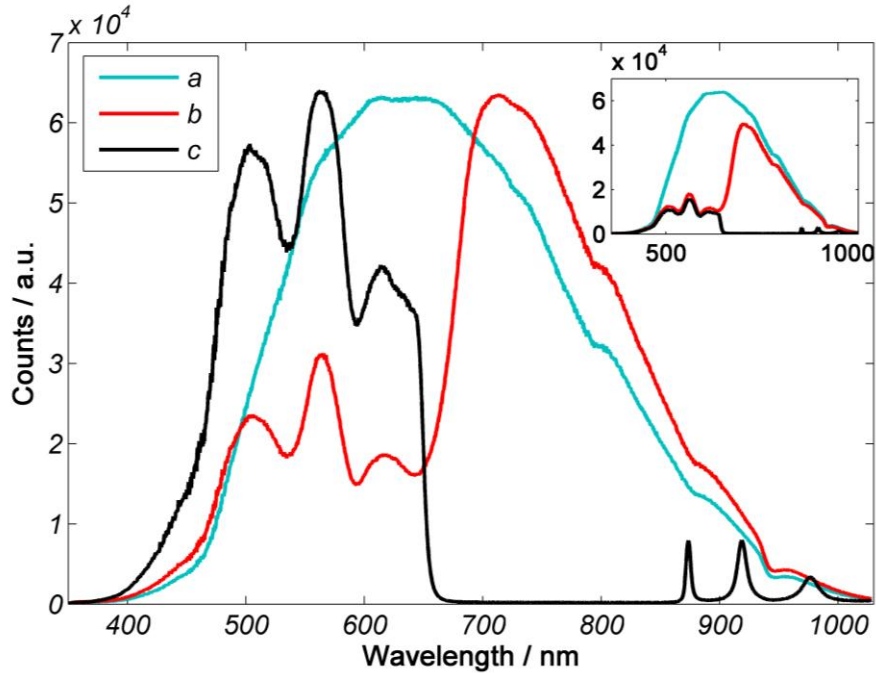


Fig. 3. The measured output of the tungsten-halogen lamp with (a) no filter, (b) color filter QB2, and (c) QB2 and SP650 (short pass filter). The inset shows the intensity changes after inserting the filters.

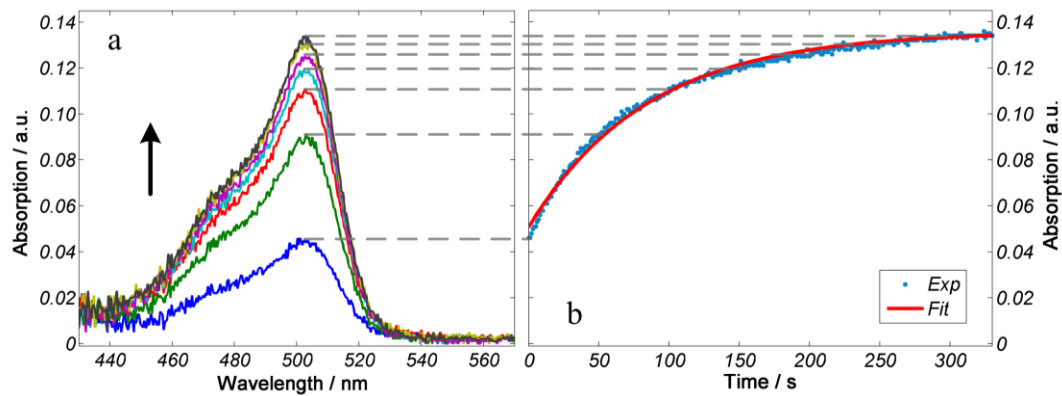


Fig. 4. The absorption spectrum of Dronpa changes with time during the photoactivation process (a) and the evolution of peak absorption at 503 nm wavelength versus time can be fitted well with a first-order kinetic model (b).

The light-activated trans-cis isomerization of Dronpa was performed under 400 nm excitation from a frequency-doubled femtosecond Ti:sapphire laser at a power of 1.7 mW/cm^2 . During the light-activation process, changes in the absorption spectra of Dronpa were recorded simultaneously and shown in Fig. 4. It was found that the absorption at 503 nm increased rapidly in the early period of time then gradually saturated and reached a constant value. By

fitting the time evolution of the peak absorbance with a first-order kinetic model, the photoswitching rate constant was calculated to be $1.17 \times 10^{-2} \text{ s}^{-1}$, which is comparable to the reported value of $9.6 \times 10^{-3} \text{ s}^{-1}$ using 405 nm 1 mW/cm² picosecond laser by Hofkens et al [10]. And in their paper, the time evolution at absorbance 388 nm was also monitored and the photoswitching rate constant at 388 nm was found to be almost the same compared to that for 503 nm [10]. This is understandable since both the disappearance of the trans state and the appearance of the cis state are from the same light-activation laser. In our experiments, the absorption at 388 nm could not be monitored due to the poor SNR in the wavelength shorter than 440 nm.

It was reported that the trans-cis photo-isomerization of Dronpa depends on the activation light intensity [6]. Therefore, the time evolution of the absorption spectrum of Dronpa under different irradiation intensity was measured and are shown in Fig. 5, and the time evolution of the peak absorbance at 503 nm was calculated and is shown in Fig. 5. Note that all the light-activation experiments were repeated three times and the data in Fig. 5 are from representative measurements. After fitting the time evolution of the peak absorbance with a first-order kinetic model, the photoswitching rate constants at different irradiance intensity could be obtained and is shown in Fig. 6. A linear dependence of the photoswitching rate constant on the irradiation intensity verifies that the light-activated trans-cis photo-isomerization is from a single photon absorption process, which is consistent with the result by Hofkens et al [10]. Moreover, the slope of the activation-intensity-dependent photoswitching rate constant (Fig. 6) was calculated to be $5.27 \times 10^{-3} \text{ cm}^2 \text{ mW}^{-1} \text{ s}^{-1}$, compared to the reported value of $1.09 \times 10^{-3} \text{ cm}^2 \text{ mW}^{-1} \text{ s}^{-1}$ obtained from a complicated fluorescence-based approach [6]. This finding proves the validity of our absorption-based approach.

Finally, it is useful to estimate the capacity of our fiber-optic system in monitoring fast photoactivation dynamics. Notice that the HL-2000-FHSA-LL tungsten-halogen lamp emits more than 1×10^5 counts per ms of integration time in the wavelength range between 400 nm and 800 nm [20]. With the use of proper ND and color filters, the USB2000+ spectrometer could easily collect 1×10^4 counts signals from the lamp with an integration time of 1 ms. Actually, when the integration time is set to be 1 ms and the number of signal averaging is set to be 5, the time evolution of absorption spectrum between 400 nm and 800 nm could be monitored every 10 ms (as shown in the inset of Fig. 5 (b)), where the minimum measurable absorption change is

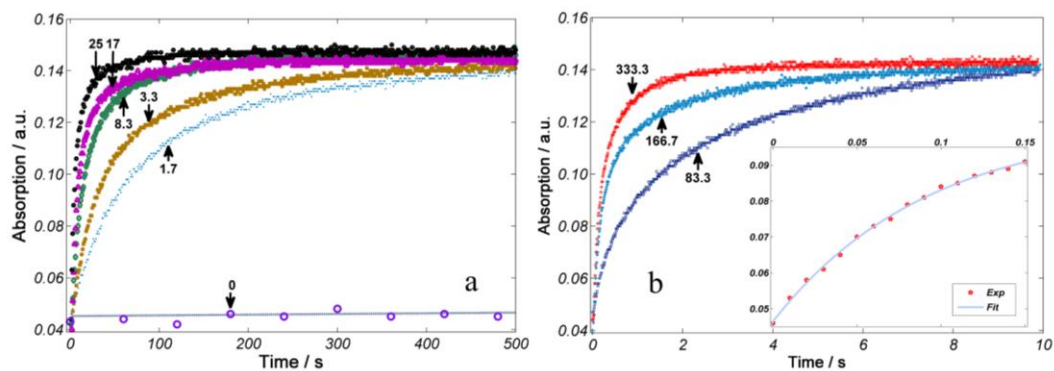


Fig. 5. Time evolution of Dronpa's peak absorption during the activation process under low (a) and high (b) intensity of activation light (mW cm^{-2}). Note that under high activation intensities, the absorption changes were recorded every 10 ms (see the inset of (b), which is for an activation intensity of 333.3 mW cm^{-2}).

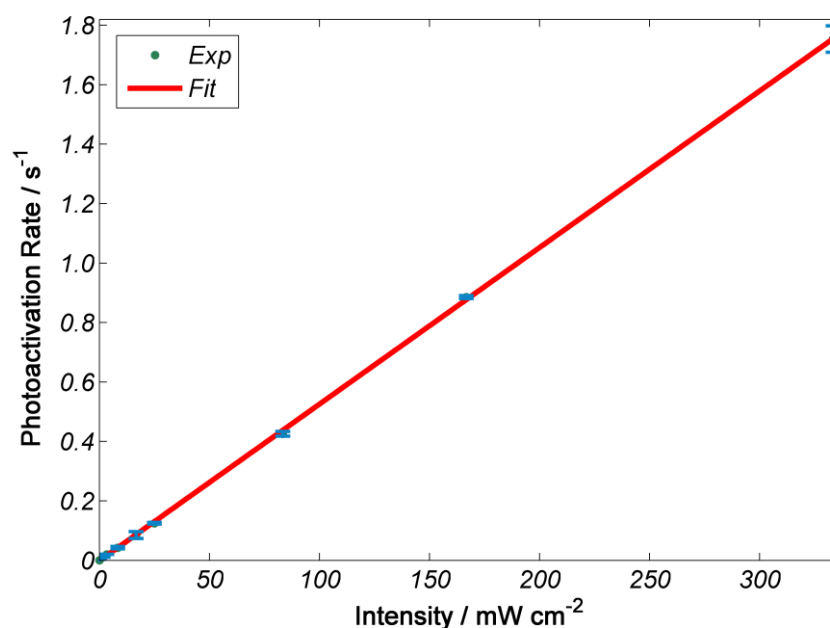


Fig. 6. The photoswitching rate constant depends linearly on the intensity of activation light. Note that the data points are from the mean of three independent experiments, and the reproducibility of these experiments is shown with the error bars.

about 3×10^{-3} . In addition, replacing the tungsten-halogen light source used in our setup with a halogen-deuterium light source could extend the wavelength range of our setup to as short as 250 nm [21].

4. Conclusion

In this paper, we have introduced a fiber-optic system for monitoring fast photoactivation dynamics of optical highlighter proteins. Using Dronpa as a representative highlighter protein and the 400 nm light from a frequency-doubled femtosecond Ti:sapphire laser as the activation source, we have demonstrated that this system is capable of recording time evolution of the absorption spectrum of Dronpa between 440 nm and 650 nm, where the interval between two absorption spectra is less than one second and the minimum measurable absorption is 2.89×10^{-3} . Moreover, we have found that it is necessary to include suitable color filters in the optical setup, otherwise the intensity accuracy in the absorption spectrum measurement could not be guaranteed. Finally, we show that this fiber-optic system is capable of monitoring absorption changes of about 3×10^{-3} at every 10 ms, which is of great benefit for the development of fast PALM.

Acknowledgments

This work was supported by the National Basic Research Program of China (2011CB910401) and the National Natural Science Foundation of China (Grant Nos. 30970691 and 30925013), and the Program for New Century Excellent Talents in University of China (Grant No. NCET-10-0407). We thank Dr. A. Miyawaki for the Dronpa plasmid and appreciate technical support from the Analytical and Testing Center of Huazhong University of Science and Technology.